Southeast-Asian J. of Sciences: Vol. 1, No 2(2012) pp. 176-194

A SIMPLE CONTROLLER FOR TWO WHEELED WELDING MOBILE MANIPULATOR

Manh Dung Ngo* and **Xuan Khoat Ngo†**

**Nguyen Tat Thanh University*
Ho Chi Minh City, Vietnam
e-mail: nmdung@ntt.edu.vn

†Ba Ria - Vung Tau Province Vocational Training College
Vung Tau, Vietnam
e-mail: khoatbrvtpvc@gmail.com

Abstract

A three-linked manipulator mounted on a two-wheeled mobile platform is used to weld a long curved welding path. A welding torch mounted at the end of a manipulator of the welding mobile manipulator (WMM) must be controlled for tracking a welding path with constant velocity and constant welding angle of torch. In this paper, a decentralized control method is applied to control the WMM considered as two separate subsystems such as a mobile platform and a manipulator. Two decentralized motion controllers are designed to control two subsystems of WMM, respectively. Firstly, based on a tracking error vector of the manipulator and a feedback motion of the mobile platform, a kinematic controller is designed for manipulator. Secondly, based on an another tracking error vector of the mobile platform and a feedback angular velocities of revolution joints of three-link, a sliding mode controller is designed for the mobile platform. These controllers are obtained based on the Lyapunovs function and its stability condition to ensure for the tracking error vectors to be asymptotically stable. Furthermore, simulation and experimental results are presented to illustrate the effectiveness of the proposed algorithm.

Key words:manipulator, mobile platform, decentralized motion controller, kinematic controller, sliding mode controller, Lyapunovs function.

1. Introduction

Nowadays, the welding robots become widely used in the tasks which are harmful and dangerous for the welders. A good welding robot used in welding application can generates the perfect movements at a certain travel speed and reference welding angle of torch, which can produce a consistent weld penetration and weld strength. In practice, some various robotic welding systems have been developed recently. Kim, et al. (2000) developed a three dimensional laser vision system for an intelligent shipyard welding robot to detect the welding position and to recognize the 3D shape of the welding environments. Jeon, et al. (2002) presented the seam tracking and motion control of a two-wheeled welding mobile robot for lattice welding. The control is separated into three driving motions: straight locomotion, turning locomotion, and torch slider control. Ngo, et al. (2006) proposed a sliding mode control of two wheeled welding mobile robot for tracking a smooth-curved path.

As we know, the welding mobile robot (WMR) is more simple system than WMM. But its welding point has three degree of freedom (d.o.f.) which is under condition of nonholonomic system of a two-wheeled mobile platform. For this reason, the WMR cannot eliminate its tracking errors and satisfies the welding condition as the same time. It only achieves the welding condition when its tracking errors are zero.

To solve this problem, a WMM of three d.o.f. independent to its two-wheeled mobile platform is considered. The developed WMM consists of a three-linked manipulator plus a two-wheeled mobile platform (MP). The mobile manipulator is used for increasing the d.o.f. of the welding point. Hence it satisfies the constraints of the welding task. In this paper, the WMM is considered as two separate subsystems such as a MP and a manipulator. Two decentralized motion controllers are applied to control two subsystems of WMM, respectively. Based on a tracking error vector which is achieved from difference between a real posture of torch and its reference one, and feedback motions of MP, a kinematic controller is designed for manipulator to carry the welding torch for tracking a reference welding path with a constant velocity and a constant reference welding angle. The mobile platform is used to carry the manipulator to avoid its singularities. So the movement of the MP is specified. In this application, the MP is controlled by a sliding mode controller in order to make the manipulators configuration return to its good posture configuration. The good posture of manipulator is defined in next section. Based on this idea, another error vector for a sliding mode controller of the mobile platform is obtained from difference between a real posture of the manipulator and its good-posture.

A developed WMM is shown in Fig. 1. The three-linked manipulator is mounted on the center of the MP. An angle sensor of link is attached at its revolution joint. The MP has more two passive wheels which are installed in

front and rear at the bottom of MP for its balance, and their motion can be ignored in the dynamics. The motion of two wheels of MP is measured by rotation encoders. The touch sensor is fixed at the end of a third-link as shown in Fig. 1.

The touch sensor rolls along a steel wall to detect the tracking errors. A simple way of measuring the errors by potentiometers is introduced in experimental result part. To illustrate the effectiveness of the proposed algorithm, simulation and experimental results are presented.

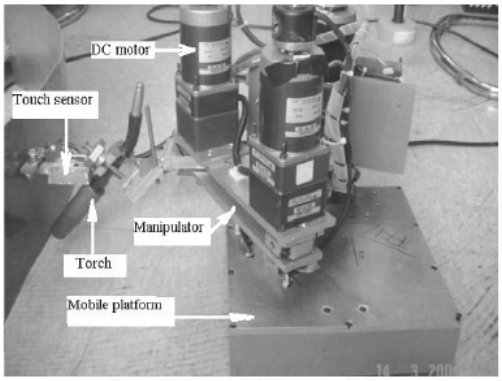

Fig. 1 The welding mobile manipulator

2. Modeling of Mobile Manipulator

2.1 Modeling of the mobile platform

Consider a WMM as shown in Fig. 2. It is model under the following assumptions:

• The MP has two driving wheels for body motion, and those are positioned on an axis passed through its geometric center,

• The three-linked manipulator is mounted on the geometric center of the MP,

• The distance between the mass center and the rotation center of the MP is . Fig. 2 doesnt show this distance. This value will be presented in the dynamic equation of MP.

• A magnet is set up at the bottom of the WMM to avoid slipping.

Fig. 2 Scheme for deriving the kinematic equations of the welding mobile manipulator

In Fig. 2, (X_P, Y_P) is a center coordinate of the MP, Φ_P is heading angle of the MP, ω_{rw}, ω_{lw} are angular velocities of the right and the left wheels,

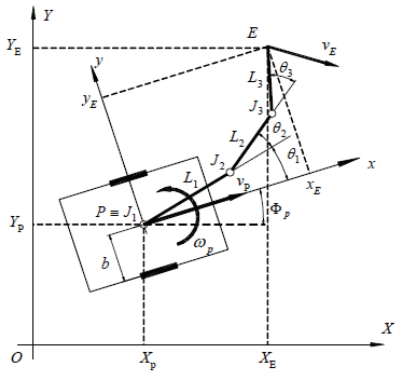

Fig. 2 Scheme for deriving the kinematic equations of the welding mobile manipulator

$\tau = \left[\tau_{rw}\ \tau_{tw}\right]^T$ is torques vector of the motors acting on the right and the left wheels, $2b$ is distance between driving wheel, r is radius of driving wheel, m_c is mass of the WMM without the driving wheels, m_w is mass of each driving wheel with its motor, I_w is moment of inertia of wheel and its motor about the wheel axis, I_m is moment of inertia of wheel and its motor about the wheel diameter axis and I_c is moment of inertia of the body about the vertical axis through the mass center.

Consider a robot system having an n-dimensional configuration space with generalized coordinate vector $\mathbf{q} = (q_1, \ldots, q_n)$ and subject to m constraints of the following form:

$$\mathbf{A}(\mathbf{q})\dot{\mathbf{q}} = 0 \tag{1}$$

where $\mathbf{A}(\mathbf{q}) \in \mathbb{R}^{m\times n}$ is the matrix associated with the constraints.

As a result, the kinematic model under the nonholonomic constraints in (1) can be derived as follows:

$$\dot{\mathbf{q}} = \mathbf{J}(\mathbf{q})\mathbf{z} \tag{2}$$

where $\mathbf{J}(\mathbf{q})$ is a $n \times (n-m)$ full rank matrix satisfying $\mathbf{J}^T(\mathbf{q})\ \mathbf{A}^T(\mathbf{q}) = 0$, and $\mathbf{z} \in \mathbb{R}^{n-m}$ is velocity vector.

Firstly, the posture of MP for the center point $P(X_P, Y_P)$ in the Cartesian space in Fig. 2 is defined as

$$\mathbf{q} = [X_P, Y_P, \Phi_P]^T \tag{3}$$

If the mobile robot has nonholonomic constraint that the driving wheels purely roll and do not slip, $\mathbf{A}(\mathbf{q})$ in (1) can be expressed into

$$\mathbf{A}(\mathbf{q}) = \left[-\sin\Phi_P\ \cos\Phi_P\ 0\right] \tag{4}$$

From (3) and (4), $n = 3$ and $m = 1$.

The velocity vector in (2) is defined as

$$\mathbf{z} = \begin{bmatrix} \nu_P \, \omega_P \end{bmatrix}^T \tag{5}$$

In the kinematic model of (2), $\mathbf{J}(\mathbf{q})$ is written as

$$\mathbf{J}(\mathbf{q}) = \begin{bmatrix} \cos\Phi_P & 0 \\ \sin\Phi_P & 0 \\ 0 & 1 \end{bmatrix} \tag{6}$$

The relationship between ν, ω and the angular velocities of two driving wheels is given by

$$\begin{bmatrix} \omega_{rw} \\ \omega_{lw} \end{bmatrix} = \begin{bmatrix} 1/r & b/r \\ 1/r & -b/r \end{bmatrix} \begin{bmatrix} \nu_P \\ \omega_P \end{bmatrix} \tag{7}$$

In this application, the welding speed is very slow so that the manipulator motion during the transient time is assumed as a disturbance for MP. For this reason, the dynamic equation of the MP under nonholonomic constraints in (1) is described by Euler-Lagrange formulation as follows:

$$\mathbf{M}(\mathbf{q})\ddot{\mathbf{q}} + \mathbf{V}(\mathbf{q}, \dot{\mathbf{q}})\dot{\mathbf{q}} = \mathbf{B}(\mathbf{q})\tau - \ \mathbf{A}^T(\mathbf{q})\lambda \tag{8}$$

where $\mathbf{M}(\mathbf{q}) \in \mathbb{R}^{n \times n}$ is a symmetric positive definite inertia matrix, $\mathbf{V}(\mathbf{q}, \dot{\mathbf{q}}) \in \mathbb{R}^{n \times n}$ is a centripetal and Coriolis matrix, $\mathbf{B}(\mathbf{q}) \in \mathbb{R}^{n \times r}$ is an input transformation matrix, $\mathbf{A}(\mathbf{q}) \in \mathbb{R}^{m \times n}$ is a matrix of nonholonomic constraints, $\tau \in \mathbb{R}^r$ is a control input vector, and $\lambda \in \mathbb{R}^m$ is a constraint force vector. For simplicity of analysis, it is assumed that $r = n - m$.

Differentiating (2), substituting this result to (8) and multiplying by $\mathbf{JT}$, (8) is rewritten as follows:

$$\mathbf{J}^T\mathbf{M}\mathbf{J}\dot{\mathbf{z}} + \mathbf{J}^T(\mathbf{M}\dot{\mathbf{J}} + \mathbf{V}\mathbf{J})\mathbf{z} = \mathbf{J}^T\mathbf{B}\tau \tag{9}$$

Multiplying by (9) can be rewritten as follows:

$$\overline{\mathbf{M}}(\mathbf{q})\dot{\mathbf{z}} + \overline{\mathbf{V}}(\mathbf{q}, \dot{\mathbf{q}})\mathbf{z} = \tau \tag{10}$$

where

$\bar{\mathbf{M}}(\mathbf{q}) = \mathbf{J}^T\mathbf{B})^{-1}\mathbf{J}^t\mathbf{M}\mathbf{J} \in \mathbb{R}^{r \times (n-m)}$,

$\bar{\mathbf{V}}(\mathbf{q}, \mathbf{z}) = (\mathbf{J}^T\mathbf{B})^{-1}\mathbf{J}^T(\mathbf{M}\mathbf{J} + \mathbf{V}\mathbf{J}) \in \mathbb{R}^{n \times (n-m)}$,

$$\bar{\mathbf{V}} = \begin{bmatrix} 0 & \frac{r^2}{2b} m_c d\dot{\Phi} \\ -\frac{r^2}{2b} m_c d\dot{\Phi} & 0 \end{bmatrix},$$

$$\bar{\mathbf{M}} = \begin{bmatrix} \frac{r^2}{4b^2}(mb^2 + I) + I_w & \frac{r^2}{4b^2}(mb^2 - I) \\ \frac{r^2}{4b^2}(mb^2 - I) & \frac{r^2}{4b^2}(mb^2 + I) + I_w \end{bmatrix},$$

$m = m_c + 2m_w,\ I = m_c d^2 + 2m_w b^2 + I_c + 2I_m.$

In practices, the dynamic equation of the MP under disturbance and interaction between the manipulator and the MP is expressed as follows:

$$\overline{\mathbf{M}}(\mathbf{q})\dot{\mathbf{z}} + \overline{\mathbf{V}}(\mathbf{q}, \dot{\mathbf{q}})\mathbf{z} + \mathbf{F}_d = \tau \tag{11}$$

where $\mathbf{F}_d$ is the disturbance and interaction between manipulator and MP. $\mathbf{F}_d$ is bounded and is represented in anther way as follows [Chwa , et al.]:

$$\mathbf{F}_d = \overline{\mathbf{M}}(\mathbf{q})\mathbf{f} \tag{12}$$

where $\mathbf{f} \in \mathbb{R}^{(n-m)\times 1}$.

On the other hand, the dynamic equation of MP can be expressed by a feedback linearization of the system as follows (Yang and Kim, 1999)

$$\tau = \overline{\mathbf{M}}(\mathbf{q})\dot{\mathbf{z}}_r + \overline{\mathbf{V}}(\mathbf{q}, \dot{\mathbf{q}})\mathbf{z} + \overline{\mathbf{M}}(\mathbf{q})\mathbf{u}_{mb} \tag{13}$$

where $\mathbf{z}_r \in \mathbb{R}^{(n-m)\times 1}$ is a reference input vector, and $\mathbf{u}_{mb} \in \mathbb{R}^{(n-m)\times 1}$ is a controller vector which is defined by computed torque method.

From Eqs. (11, 12 and 13), this relationship yields.

$$\mathbf{f} - \mathbf{u}_{mb} = -(\dot{\mathbf{z}} - \dot{\mathbf{z}}_r) \tag{14}$$

2.2 Modeling of the 3 links manipulator

Consider a three-linked manipulator as shown in Fig. 2. A new Cartesian coordinate frame (Frame $x - y$) is fixed on the mobile platform as shown in Fig. 2. The (Frame $x - y$) is called the moving coordinate frame because this coordinate frame is moved toghether with the mobile platform in the world coordinate (frame $X - Y$). The velocity vector of the end-effector with respect to the moving frame is given by

$$^1\mathbf{V}_E = \mathbf{J}\dot{\Theta} \tag{15}$$

where $^1\mathbf{V}_E = \begin{bmatrix}\dot{x}_E & \dot{y}_E & \dot{\phi}_E\end{bmatrix}^T$ is the velocity vector of the end-effector with respect to the moving frame, $\dot{\Theta} = \begin{bmatrix}\dot{\theta}_1 & \dot{\theta}_2 & \dot{\theta}_3\end{bmatrix}^T$ is the angular velocity vector of the revolution joints of the three-linked manipulator, and $\mathbf{J}$ is the Jacobian matrix.

$$\mathbf{J} = \begin{bmatrix} -L_3S_{123} - L_2S_{12} - L_1S_1 & -L_3S_{123} - L_2S_{12} & -L_3S_{123} \\ L_3C_{123} + L_2C_{12} + L_1C_1 & L_3C_{123} + L_2C_{12} & L_3C_{123} \\ 1 & 1 & 1 \end{bmatrix} \tag{16}$$

where L_1, L_2, L_3 are the length of links of the manipulator, and

$S_1 = \sin(\theta_1), S_{12} = \sin(\theta_1 + \theta_2), S_{123} = \sin(\theta_1 + \theta_2 + \theta_{31})$,
$C_1 = \cos(\theta_1), C_{12} = \cos(\theta_1 + \theta_2), C_{123} = \cos(\theta_1 + \theta_2 + \theta_{31})$

The dynamic equation of the end-effector of the manipulator with respect to the world frame is obtained as follows [Lewis, et al.]:

$$\mathbf{V}_E = \mathbf{V}_P + \mathbf{W}_P \times {}^0\mathbf{Rot}_1 {}^1\mathbf{P}_E + {}^0\mathbf{Rot}_1 {}^1\mathbf{V}_E \tag{17}$$

where $\mathbf{V}_E$ and $\mathbf{V}_P$ are the velocity vector of the end-effector and the velocity vector of the center point of platform with respect to the world frame, respectively. $\mathbf{W}_P$ is the rotational velocity vector of the moving frame. ${}^0\mathbf{Rot}_1$ is the rotation transform matrix from the moving frame to the world frame. ${}^1\mathbf{P}_E$ is the position vector of the end-effector with respect to the moving frame

$$\mathbf{V}_E = \begin{bmatrix} \dot{X}_E \\ \dot{Y}_E \\ \dot{\Phi}_E \end{bmatrix}, \mathbf{V}_P = \begin{bmatrix} \dot{X}_P \\ \dot{Y}_P \\ \dot{\Phi}_E \end{bmatrix}, \mathbf{W}_P = \begin{bmatrix} 0 \\ 0 \\ \dot{\Phi}_P \end{bmatrix}, \mathbf{P}_E = \begin{bmatrix} x_E \\ y_E \\ \phi_E \end{bmatrix},$$

$${}^1\mathbf{P}_E = [L_1C_1 + L_1C_{12} + L_3C_{123} \quad L_1S_1 + L_2S_{12} + L_3S_{123} \quad \phi_E]^T$$

$${}^0\mathbf{Rot}_1 = \begin{bmatrix} \cos\Phi_P & -\sin\Phi_P & 0 \\ \sin\Phi_P & \cos\Phi_P & 0 \\ 0 & 0 & 1 \end{bmatrix},$$

$$\Phi_E = \theta_1 + \theta_2 + \theta_3 + \Phi_E - \tfrac{\pi}{2}, \quad \dot{\Phi}_E = \dot{\theta}_1 + \dot{\theta}_2 + \dot{\theta}_3 + \dot{\Phi}_P.$$

3. Decentralized Controllers Design

In this section, a decentralized control method is applied. A sliding mode controller and a kinematic controller are used to control the MP and the manipulator of WMM, respectively. The relationship between two controllers can be expressed as follows: Firstly, based on a tracking error vector which is obtained from difference between a real posture of torch and a reference one, and feedback motions of mobile platform, a kinematic controller is designed for the manipulator in order to move the welding torch tracking a welding path. Secondly, the mobile platform is used to carry the manipulator to avoid its singularities. So the movement of the MP is specified. For this reason, another error vector is obtained from difference between a real posture and the good-posture of the manipulator. Based on this error vector, a new sliding mode controller is applied to control two wheeled mobile platform. These controllers are obtained based on the Lyapunovs function and its stability condition to ensure for the error vectors to be asymptotically stable.

3.1 Kinematic controller design for manipulator

From Fig. 3, the tracking error vector $\mathbf{E}_T$ is defined as follows:

$$\mathbf{E}_T = \begin{bmatrix} e_1 \\ e_2 \\ e_3 \end{bmatrix} = \begin{bmatrix} \cos\Phi_E & \sin\Phi_E & 0 \\ -\sin\Phi_E & \cos\Phi_E & 0 \\ 0 & 0 & 1 \end{bmatrix} \begin{bmatrix} X_R - X_E \\ Y_R - Y_E \\ \Phi_R - \Phi_E \end{bmatrix} \tag{18}$$

The tracking error vector can be rewritten in the matrix form as follows:

$$\mathbf{E}_T = \mathbf{A}[P_R - P_E] \tag{19}$$

where $\mathbf{A} = \begin{bmatrix} \cos\Phi_E & \sin\Phi_E & 0 \\ -\sin\Phi_E & \cos\Phi_E & 0 \\ 0 & 0 & 1 \end{bmatrix}$ and $P_R = (X_R \ Y_R \ \Phi_R)^T$ is a reference welding point which is moved along the welding path with a constant velocity and constant welding angle. $P_R = (X_E \ Y_E \ \Phi_E)^T$ is a welding point or an end-effector point.

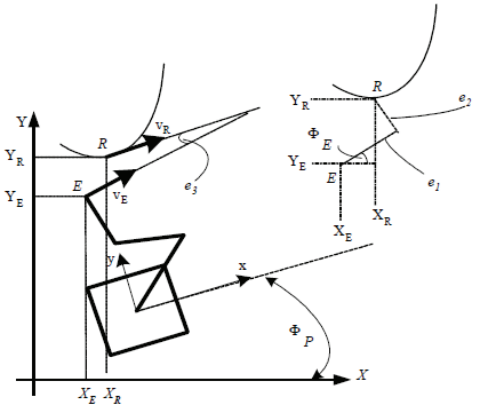

Fig. 3 Scheme for deriving the tracking error vector $\mathbf{E}_T$ of manipulator

error vector $\mathbf{E}_T$ of manipulator

The first derivative of tracking error vector $\mathbf{E}_T$ yields

$$\dot{\mathbf{E}}_T = \dot{\mathbf{A}}(\mathbf{p}_R - \mathbf{p}_E) + \mathbf{A}(V_R - \mathbf{V}_E) \tag{20}$$

$$\dot{\mathbf{E}}_T = \begin{bmatrix} \dot{e}_1 \\ \dot{e}_2 \\ \dot{e}_3 \end{bmatrix} = \begin{bmatrix} \omega_E e_2 - \nu_E + \nu_R \cos e_3 \\ -\omega_E e_1 + \nu_R \sin e_3 \\ \omega_R - \omega_E \end{bmatrix} \tag{21}$$

To obtain the kinematic controller a back stepping method is used. The Lyapunove function is proposed as follows:

$$\mathbf{V}_0 = \frac{1}{2}\mathbf{E}_T^T\mathbf{E}_T \tag{22}$$

The first derivative of $\mathbf{V}_0$ yields

$$\dot{\mathbf{V}}_0 = \mathbf{E}_T^T \tag{23}$$

To achieve the negativeness of $\dot{\mathbf{V}}_0$, the following equation must be satisfied

$$\dot{\mathbf{E}}_T = -\mathbf{K}\mathbf{E}_T \tag{24}$$

where $\mathbf{K} = \text{diag}(k_1,\ k_2\ k_3)$ with k_1, k_2 and k_3 are the positive constants. Substituting (15), (17) and (20) into (24) yields

$$-\mathbf{K}\mathbf{E}_T = \ \dot{\mathbf{A}}\ \mathbf{A}^{-1}E_T + \ \mathbf{A}(\mathbf{V}_R - (V_P + \mathbf{W}_P \times {}^0\mathbf{Rot}_1\,{}^1\mathbf{p}_E + {}^0\mathbf{Rot}_1\mathbf{J}\dot{\Theta})) \tag{25}$$

The error vector E_T converges to zero when there is a controller $\mathbf{u}_{mP} = [u_{1mp}\ u_{2mp}\ u_{3mp}]^T$ such that the angular velocity vector $\dot{\Theta}$ of the revolution joints satisfy the following condition.

$$\mathbf{u}_{mp} = \dot{\Theta} = \mathbf{J}^{-1\,0}\mathbf{Rot}_1^{-1}(\mathbf{A}^{-1}(\dot{\mathbf{A}}\ \mathbf{A}^{-1} + \mathbf{K})\mathbf{E}_T + \mathbf{V}_R - \mathbf{V}_P - \mathbf{W} \times {}^0\mathbf{Rot}_1\,{}^1\mathbf{p}_E. \tag{26}$$

The controllers vector $\mathbf{u}_{mp}$ is rewritten in another form as follows:

$$\begin{aligned} u_{mp} = \dot{\theta}_1 = \ & \tfrac{1}{L_1 S_2}\big\{\nu_R S_{3e_3} - \nu_P C_{12} + (e_2k_2 - e_1\omega_E)C_3 \\ & + [e_1k_1 + e_2\omega_E + L_3(\omega_R + e_3(k_3 + \omega_E))]S_3\big\} - \omega_P \end{aligned} \tag{27}$$

$$\begin{aligned} u_{2mp} = \dot{\theta}_2 \ & = \tfrac{1}{L_1 L_2 S_2}\big\{ - \nu_R(L_1 S_{23e_3} + L_2 S_{3e_3}) + \nu_P(L_1 C_1 + L_2 C_{12}) \\ & + (\omega_E e_1 - e_2 k_2)(L_1 C_{23} + L_2 C_3) \\ & - (L_1 S_{12} + L_2 S_3)[L_3 e_3(k_3 + \omega_E) + L_3\omega_R + e_1k_1 + e_2\omega_E]\big\} \end{aligned} \tag{28}$$

$$\begin{aligned} u_{3mp} = \dot{\theta}_3 \ & = \tfrac{1}{L_2 S_2}\big\{\nu_R S_{23e_3} + (e_2k_2 - e_1\omega_E)C_{23} - \nu_P C_1 + [e_2\omega_E \\ & + k_1e_1 + L_3(\omega_R + e_3(k_3 + \omega_E))]S_{23}\big\} + (\omega_R + e_3(k_3 + \omega_E)) \end{aligned} \tag{29}$$

where $S_{23e_3} = \sin(\theta_2 + \theta_3 + e_3);\ S_{3e_2} = \sin(\theta_3 + e_3)$.

3.2 Dynamic controller design for mobile platform

In this part, a sliding mode is used to bring the configuration of the manipulator to good posture. The good posture of manipulator is chosen with $\theta_1 = \frac{\pi}{4}, \theta_2 = \frac{\pi}{2}, \theta_3 = -\frac{\pi}{4}$.

Let a point $M(X_M, Y_M, \Phi_M)$ be a fixed point with respect to the moving frame and made by the good posture of the manipulator. A sliding mode controller is proposed to control the MP for the point M tracking the real reference point E . When the point M coincides with point E, that is it means that the manipulator has the good configuration for avoiding its singularity. Coordinate of the point is expressed as follows:

$$X_M = X_P - D\sin\Phi_P; \quad Y_M = Y_P + D\cos\Phi_P; \quad \Phi_M = \Phi_P \tag{30}$$

where $D = L_1\sin(\frac{\pi}{4} + L_2\sin(\frac{\pi}{2}) + L_3\sin(-\frac{\pi}{4})$.

The derivative of (30) is as follows

$$\dot{X}_M = \nu_P\cos\Phi_P - D\omega_P\cos\Phi_P; \dot{Y}_M = \nu_P\sin\Phi_P - D\omega_P\sin\Phi_P; \dot{\Phi}_M = \omega_P. \tag{31}$$

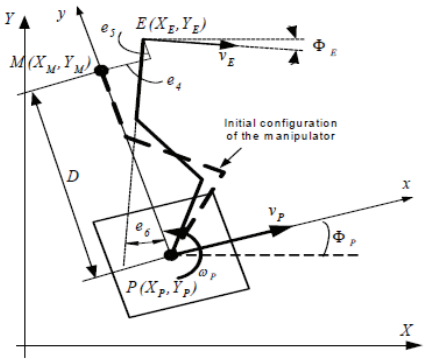

Fig. 4 Scheme for deriving the MP tracking error vector

A new tracking error vector $\mathbf{E}_{mb}$ for MP is defined as follows:

$$\mathbf{E}_{mb} = \begin{bmatrix} e_4 \\ e_5 \\ e_6 \end{bmatrix} = \begin{bmatrix} \cos\Phi_P & \sin\Phi_P & 0 \\ -\sin\Phi_P & \cos\Phi_P & 0 \\ 0 & 0 & 1 \end{bmatrix} \begin{bmatrix} X_E - X_M \\ Y_E - Y_M \\ \Phi_E - \Phi_M \end{bmatrix} \tag{32}$$

where $\Phi_E = \Phi_r + e_3$.

Let ν_P, ω_P, ν_E and ω_E, be the linear velocity, the angular velocity of the MP, the linear velocity and the angular velocity of the end-effector with respect to the world frame, respectively. Then the derivative of MP error vector yields.

$$\begin{bmatrix} \dot{e}_4 \\ \dot{e}_5 \\ \dot{e}_6 \end{bmatrix} = \begin{bmatrix} \nu_E\cos e_6 - \nu_P + e_5\omega_P + D\omega_P \\ \nu_E\sin e_6 - e_4\omega_P \\ -(\omega_P - \omega_r) + \dot{e}_3 \end{bmatrix} \tag{33}$$

The following part presents a sliding mode controller vector $\mathbf{u}_{mb}$. This controller designs the torque of DC motor for two driven wheels of mobile platform in order to make the MP error vector converge to zero.

3.2.1 Sliding mode controller design

To design a sliding mode controller, the sliding surfaces are defined as follows:

$$\mathbf{s} = \begin{bmatrix} s_1 \\ s_2 \end{bmatrix} = \begin{bmatrix} \dot{e}_4 + k_4 e_4 \\ \dot{e}_6 + k_6 e_6 + k_5 \psi(e_6) e_5 \end{bmatrix} \tag{34}$$

where k_4, k_5 and k_6 are positive constant values. $\psi(.)$ is a bounding function and is defined as follows:

$$\psi(e_6) = \begin{cases} 0 \rightarrow 1 & \text{if } |e_6| \leq \epsilon \\ 1 \rightarrow 0 & \text{if } |e_6| \geq 2\epsilon \\ \text{no change} & \text{if } \epsilon < |e_6| < 2\epsilon \end{cases} \tag{35}$$

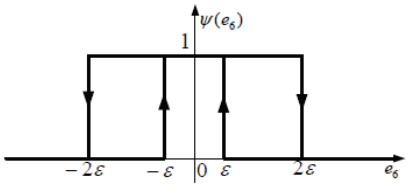

Fig. 5 Characteristic of $\psi(\cdot)$ function.

In (35) and Fig. 5, ϵ is a positive constant value. No change means that the value of $\psi(.)$ function continuously keeps its value at $e_6 = \pm\epsilon$ or $e_6 = \pm 2\epsilon$ before e_6 enters into $\epsilon < |e_6| < 2\epsilon$.

When the sliding surface vector is zero, the followings are obtained from the (32):

$$\dot{e}_4 = -k_4 e_4 \tag{36}$$

$$\dot{e}_6 = -k_6 e_6 - k_5 \psi(e_6) e_5 \tag{37}$$

In (36), if e_4 is positive, $\dot{e}_4$ is negative, and vice versa. Thus, the equilibrium point of e_4 converges to zero as $t \rightarrow \infty$. It means that the error $e_4 \rightarrow 0$ as $t \rightarrow \infty$ along the sliding surface ($s_1 = 0$).

Because the configuration of the WMR has the point M which is located on the axis through the two contact points between driving wheels and floor, the error can be eliminated via e_6. For example, if $e_4 = 0$ and $e_6 = 0$, the value of $e_5$is constant from (33). For that result, the error e_6 and its derivative in (37) cannot be zero in order to eliminate the error e_5 when the error $e_5 \neq 0$.

In case of $|e_6|$, firstly, $\psi(.)$ is un-active until $e_6 \leq \epsilon$. So (37) becomes $\dot{e}_6 = -k_6 e_6$. Similarly with (36), e_6 converges into $(-\epsilon, \epsilon)$. Secondly, when $|e_6| <$

$\epsilon, \psi(.)$ is active until $|e_6| > 2\epsilon$. So (37) becomes $\dot{e}_6 = -k_6 e_6 - k_5 e_5$. By this result, the heading angle of the platform must be changed for the derivative of the error of heading angle to be equal to $-k_6 e_6 - k_5 e_5$. While the heading angle of mobile platform is varied, the e_5 convergs to zero. When $e_5 \to 0$, (37) becomes $\dot{e}_6 = -k_6 e_6$. So $e_5 \to 0$ as $t \to \infty$.

Based on Lyapunovs function and its stability condition, a back-steeping method is used to obtain a sliding mode controller $\mathbf{u}_{mb}$. The Lyapunovs function is chosen as follows:

$$V = \frac{1}{2}\mathbf{s}^T\mathbf{s} \tag{38}$$

To satisfy the Lyapunovs stability condition $\dot{V} \leq 0$, the following proposed controller $\mathbf{u}_{mb}$ can be calculated as follows:

$$\mathbf{u}_{mb} = \begin{bmatrix} \dot{e}_5\omega_r + (e_5 + D)\dot{\omega}_r - \nu_E\dot{e}_6\text{sine}_6 \\ \dot{e}_3 \end{bmatrix} + \begin{bmatrix} k_4\dot{e}_4 \\ k_6\dot{e}_6 + k_5\psi(e_6)\dot{e}_5 \end{bmatrix} + \mathbf{Q}sgn(\mathbf{s}) + \gamma sgn(\mathbf{s}) \tag{39}$$

where $\gamma = [\gamma_1\ \gamma_2]^T$ is a positive constant value and $|\mathbf{f}| \leq \gamma$.

Proof of Lyapunov's stability condition

Because the reference welding speed is a constant $\dot{\nu}_r = 0$, from (31) and (33), the second derivatives of e_4 and e_6 yield

$$\begin{bmatrix} \ddot{e}_4 \\ \ddot{e}_6 \end{bmatrix} = \begin{bmatrix} \dot{e}_5\omega_P + (e_5 + D)\dot{\omega}_P - \nu_E\dot{e}_6\text{sine}_6 \\ \dot{e}_3 \end{bmatrix} - \begin{bmatrix} (\dot{\nu}_P - \dot{\nu}_r) \\ (\dot{\omega}_P - \dot{\omega}_r) \end{bmatrix} \tag{40}$$

Using (14), the equation (40) can be rewritten as follows:

$$\begin{bmatrix} \ddot{e}_4 \\ \ddot{e}_6 \end{bmatrix} = \begin{bmatrix} \dot{e}_5\omega_P + (e_5 + D)\dot{\omega}_P - \nu_E\dot{e}_6\text{sine}_6 \\ \dot{e}_3 \end{bmatrix} + \mathbf{f} - \mathbf{u}_{mb} \tag{41}$$

From (38), the equation (41) can be expressed as follows:

$$\begin{bmatrix} \ddot{e}_4 \\ \ddot{e}_6 \end{bmatrix} = \mathbf{f} - \mathbf{Q}\text{sgn}(\mathbf{s}) - \gamma\text{sgn}(\mathbf{s}) - \begin{bmatrix} k_4\dot{e}_4 \\ k_6\dot{e}_6 + k_5\psi(e_6)\dot{e}_5 \end{bmatrix} \tag{42}$$

From (34), the first derivative of the sliding surfaces yields

$$\dot{\mathbf{s}} = \begin{bmatrix} \ddot{e}_4 + k_4\dot{e}_4 \\ \ddot{e}_6 + k_6\dot{e}_6 + k_5\psi(e_6)\dot{e}_5 \end{bmatrix} \tag{43}$$

From (41), the first derivative of the sliding surfaces can be rewritten as follows:

$$\dot{\mathbf{s}} = \mathbf{f} - \mathbf{Q}\text{sgn}(\mathbf{s}) - \gamma\text{sgn}(\mathbf{s}) \tag{44}$$

If $|\mathbf{f}| \leq \gamma$ is chosen, the equation (39) satisfies the Lyapunovs stability condition.

$$\dot{V} = \mathbf{s}^T\dot{\mathbf{s}} \leq 0 \tag{45}$$

4. Chattering Phenomenon Elimination

In practice, a chattering phenomenon in a sliding mode control can be eliminated by a saturation function. Using the saturation function, a thin boundary layer neighboring the switching surface is achieved, and then a smooth and proper controller can be obtained.

In this case, the welding velocity is rather slow, 7.5mm/s. Therefore, a thin boundary layer $\delta = 0.1$ is chosen. A new smooth switching controller than previous switching controller in (39) can be obtained by substituting sgn(.) function to sat(.) function in (39):

$$\begin{bmatrix} u_1 \\ u_2 \end{bmatrix} = \begin{bmatrix} Q_1 & 0 \\ 0 & Q_2 \end{bmatrix} \begin{bmatrix} sat(\xi_1) \\ sat(\xi_2) \end{bmatrix} + \begin{bmatrix} \gamma_1 & 0 \\ 0 & \gamma_2 \end{bmatrix} \begin{bmatrix} sat(\xi_1) \\ sat(\xi_2) \end{bmatrix} + \begin{bmatrix} e_5\dot{\omega}_r + (e_5 + D)\omega_r - \nu_E\dot{e}_6 \mathrm{sin}e_6 \\ \dot{e}_3 \end{bmatrix} + \begin{bmatrix} k_4\dot{e}_4 \\ k_6\dot{e}_6 + k_5\psi(e_6)\dot{e}_5 \end{bmatrix} \tag{46}$$

where the saturation function is defined as

$$\begin{cases} sat(\xi_1) = sat(\frac{s_i}{\delta}) = \xi_i & \text{if } |\xi_i| \leq 1 \\ sat(\xi_i) = \mathrm{sgn}(\xi_i) & \text{otherwise} \end{cases} \tag{47}$$

With smoothing approach, the controller (39) can be implemented to the practice welding mobile robot totally. The effectiveness of the controller can be seen through the simulation and the experimental results.

5. Simulation and Experimental Results

5.1 Hardware design

5.1.1 Measurement of the errors e_1, e_2, e_3

A simple measurement scheme is implemented using potentiometers to obtain the errors e_1, e_2, e_3 as shown in Fig. 6. The experimental touch sensor is shown in Fig. 7. Two revolute potentiometers and one linear potentiometer are needed for measuring the tracking error vector. From Fig. 6, the tracking errors relations are given as

$$e_1 = -r_r \mathrm{sin}e_3; \quad e_2 = d_e + r_r \mathrm{cos}e_3; \quad e_3 = \angle(O_1E, O_1O_3) - \frac{\pi}{2} \tag{48}$$

where r_r is the radius of the rollers.

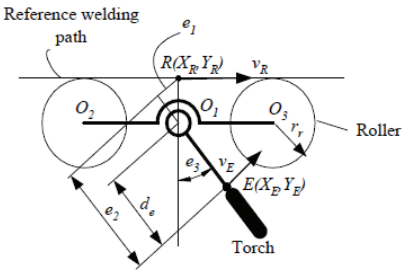

Fig. 6 The scheme of measuring errors e_1, e_2, e_3

5.1.2 Measurement of the errors e_4, e_5, e_6

From Fig. 4, the tracking errors e_4, e_5, e_6 with respect to moving frame can be calculated as follows:

$$\begin{aligned} e_4 &= x_M - x_E = L_1\cos\theta_1 - L_2\cos(\theta_1+\theta_2) - L_3\cos(\theta_1+\theta_2+\theta_3) \\ e_5 &= y_M - y_E = D - L_1\sin\theta_1 - L_2\sin(\theta_1+\theta_2) - L_3\sin(\theta_1+\theta_2+\theta_3) \\ e_6 &= \theta_1+\theta_2+\theta_3-\frac{\pi}{2} \end{aligned} \tag{49}$$

where $\Phi_E = \Phi_P + \theta_1 + \theta_2 + \theta_3 - \frac{\pi}{2}$.

The joint angles $\theta_1 + \theta_2 + \theta_3$ can be determined from the angular sensors at revolute joint of links of the manipulator.

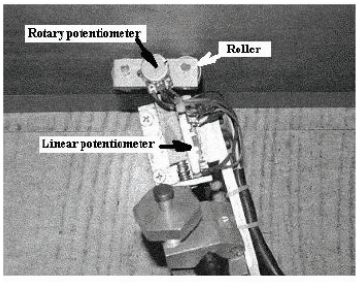

Fig. 7 The touch sensor used in experiment

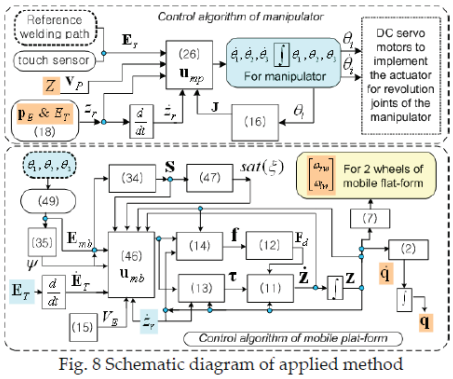

Fig. 8 Schematic diagram of applied method

5.1.3 Schematic diagram of the control algorithm of mobile manipulator

The schematic diagram for a decentralized control method is shown in Fig. 8. In this diagram, a relationship between controllers is illustrated by means of the output of this controller is one of the input ofanother controller and vice versa.

5.2 Simulation and experimental results

To verify the effectiveness of the proposed modeling and controllers, simulations and experimental results were done for the WMM with the welding reference trajectory as shown in Fig. 9. Numerical values and initial values used in simulation and experiment are shown in Table 1 and Table 2.

Table 1: Numerical and initial values for simulation

parameters	Values	Units	parameters	Values	Units
b	0.105	m	k_1	0.5	/s
r	0.025	m	k_2	0.7	/s
$L_1 = L_2 = L_3$	0.2	m	k_3	0.5	/s
ν_R	0.0075	m	k_4	2	/s
$I_c(t=0)$	0.08	m/s	k_5	3	/s
$I_W(t=0)$	$8*10^{-5}$	Kgm^2	k_6	150	/s
$I_m(t=0)$	$4*10^{-5}$	Kgm^2	$\gamma = [\gamma_1\ \gamma_2]^T$	$[30\ 35]^T$	$[\mathrm{mm}/s^2\ \ \mathrm{deg}/s^2]$
d	0.01	m	$Q = [Q_1\ Q_2]^T$	$[5\ 8]^T$	$\mathrm{mm}/s^2\ \ \mathrm{deg}/s^2$
m_W	0.2	kg	ϵ	3	deg
m_c	15	kg			

Table 2: Initial values for the simulation and experiment

Parameters	Values	Units
$[e_1\ e_2\ e_3]$	[4 6 -15]	[mm mm deg]
$[e_1\ e_2\ e_3]$	[0 0 0]	[mm mm deg]
ν_r	0.0075	m/s

Fig. 10 shows the zoom out of the end-effector for tracking the welding path at beginning. Fig. 11 shows that, with the initial tracking error values $e_1 = 6mm, e_2 = 4mm, e_3 = -15\mathrm{deg}$, the kinematic controllers of the manipulator makes this tracking error converge to zero after about 3 seconds in order to tracking the welding point. In this paper, decentralized motion control method is used, so to avoiding overshot between two controllers, the gain of controller of MP are chosen in order that a smooth welding speed is achieved. The tracking error vector $[e_4\ e_5\ e_6]^T$ which is shown in Fig. 12 converges to zero slowly. This tracking error vector doesn't directly effect on the welding result. It only helps the manipulator to avoiding its singularity. With the movement of the MP, the angle of manipulator is converted and remained in the good-posture which is shown in Fig. 13.

Fig. 14 shows that the sliding surface vector converges to zero and remains on it. Fig. 15 shows the angular velocities of right wheel and left wheel obtained by the sliding mode controller. Fig 16 shows the linear velocity of end-effector

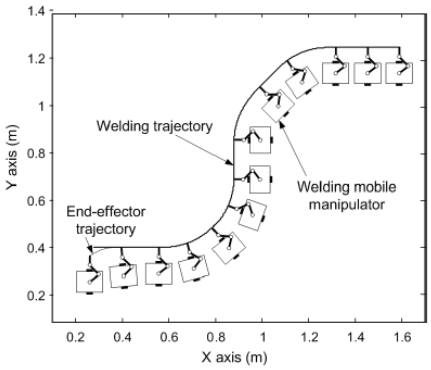

Fig. 9 The WMM is tracking along the welding path

is remained at 7.5±1 [mm] . So this welding speed is good enough for achieving a good welding result. Fig. 17 shows the simulation and experiment results of the tracking errors $[e_1\ e_2\ e_3]$ and those errors are bounded. And their average value converges to zero. Fig. 18 shows the simulation and experiment results of the tracking errors $[e_4\ e_5\ e_6]$ and those errors are bounded and also converge to zero smoothly.

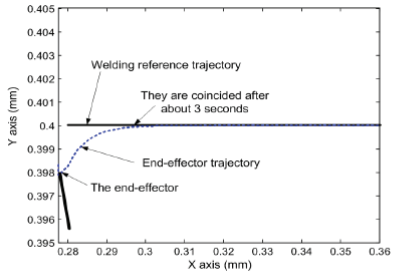

Fig. 10 Trajectory of the end-effector and its reference at beginning

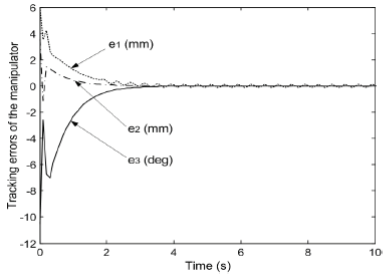

Fig. 11 Tracking errors e_1 e_2 e_3 at beginning

6. Conclusion

This paper developed a WMM which can co-work between mobile platform and manipulator for tracking a long smooth curved welding path. The main task of the control system is to control the end-effector or welding point of the WMM for tracking a welding point which is moved on the welding path with constant velocity. Furthermore, the angle of welding torch must be kept constant with respect to the welding curve. The WMM is divided into two

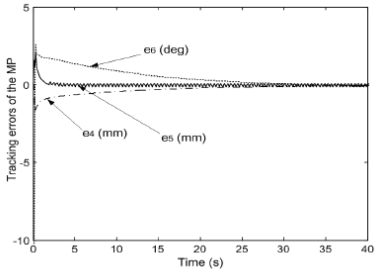

Fig. 12 Tracking errors e_4 e_5 e_6 at beginning

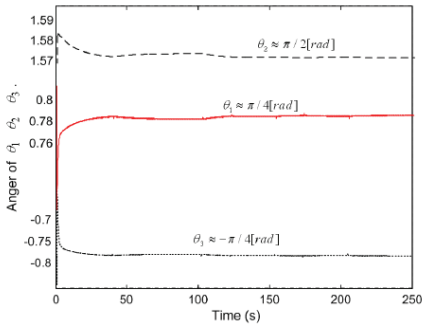

Fig. 13 Angular of revolution joints θ_1 θ_2 θ_3

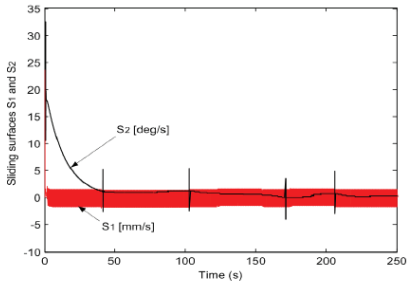

Fig. 14 Sliding surfaces s_1 s_2

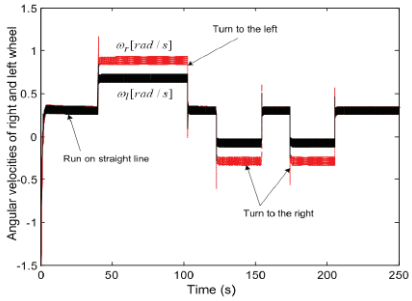

Fig. 15 Linear and angular velocities of MP

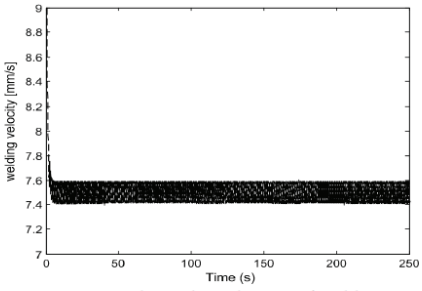

Fig. 16 Linear and angular velocities of welding point

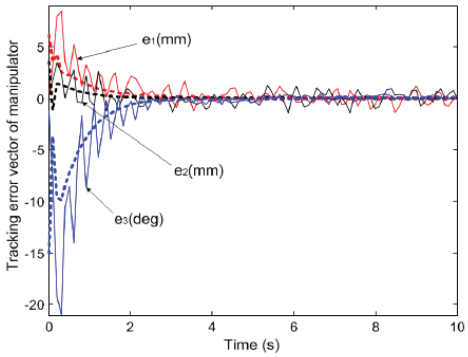

Fig. 17 Simulation and experimental results of e_1 e_2 e_3 at beginning

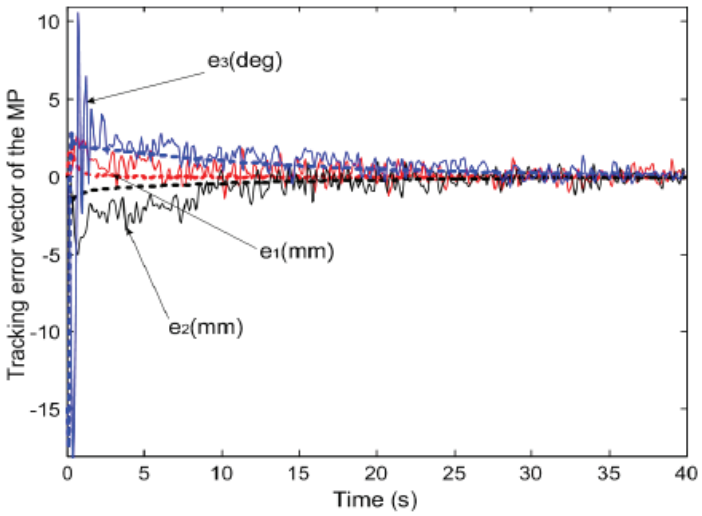

Fig. 18 Simulation and experimental results of at beginning

subsystems and is controlled by decentralized controllers. The kinematic controller and sliding mode controller are designed to control the manipulator and the mobile-platform, respectively. These controllers are obtained based on the Lyapunovs function and its stability condition to ensure the error vectors to be asymptotically stable. Furthermore, simulation and experimental results are presented to illustrate the effectiveness of the proposed algorithm. (This work was supported by Pukyong National Uni. Research Foundation Grant in 2005 (0010000200501700)

References

[1] Cheng M. P., and Tsai C. C., (2003), Dynamic Modeling and Tracking Control of a Nonholonomic Wheeled Mobile Manipulator with Two Robotic Arms, Proc. of IEEE Conference in Decision and Control, Vol. 3, pp. 2932-2937.

[2] Chwa D. K., Seo J. H., Pyojae, and Choi J. Y., (2002) Sliding Mode Tracking Control of Nonholonomic Wheeled Mobile Robots, Proc. of the American Control Conference Anchorage, pp. 3991-3996.

[3] Fierro R., and Lewis F. L., (1995) Control of a Non-holonomic Mobile Robot: Backstepping Kinematic into Dynamics, Proc. of the 34th Conf. on Decision & Control, pp. 3805 3810.

[4] Fukao T., Nakagawa H., and Adachi N., (2000) Adaptive Tracking Control of a Nonholonomic Mobile Robot, Trans. on IEEE Robotics and Automation, Vol. 16, pp. 609-615.

[5] Hootsmans N. A. M., and Dubowsky S., (1991) Large Motion Control of Mobile Manipulators Including Vehicle Suspension Characteristics, Proc. of IEEE International Conference on Robotics and Automation, Vol. 3, pp. 2336-2341.

[6] Ibanez I., Aguirre M. A., Torralba A., and Franquelo L.G., (2002) A Low Cost 3D Vision System for Positioning Welding Mobile Robots Using a FPGA Prototyping System, IEEE 28th Annual Conference of the IECON 02 on Industrial Electronics Society, Vol. 2, pp. 1590-1593.

[7] Jeon, B.Y., Park, S.S. and Kim, S.B., (2002), Modeling and Motion Control of Mobile Robot for Lattice Type of Welding, KSME International Journal, Vol. 16, No. 1, pp. 83 93.

[8] Kim M. T., Ko K. W., Cho H. S., and Kim J. H., (2000) Visual Sensing and Recognition of Welding Enviroment for Intelligent Shipyard Welding Robots, Proc. of the IEEE/RSJ

[9] Lewis F.L., Abdallah C.T., and Dawson D.M., (1993) Control of Mabot Manipulator, Ptrentice Hall International Edition.

[10] Ngo M. D., Duy V. H., Phuong N. T., and Kim S. B. (2006) Control of Two-Wheeled Welding Mobile Robot For Tracking a Smooth Curved Welding Path Proceeding of the Korean Society of Marine Engineering (KSOME) 2006 first conference, Tong-Yong City, Korea.

[11] Santos, P. G. D., Armada, M. A. and Jimenez, M. A., (2000), Ship Building with a POWER Robot, IEEE Robotics & Automation Magazine, pp. 35 43.

[12] Utkin, V., Jurgen, G., and Shi, J., (1999), Sliding Mode Control in Electromechanical Systems, E. Rogers and J. O'Reilly, Eds. London & Philadelphia: Copyright Taylor & Francis.

[13] Yang, J. M. and Kim, J. H., (1999), Sliding Mode Control for Trajectory Tracking of Nonholonomic Wheeled Mobile Robots, IEEE Trans. Robotics and Automation, Vol. 15, No. 3, pp. 578 587.